

Systematic multiconfiguration-Dirac-Fock study of the x-ray spectra accompanying the ionization in collision processes: The structure of the $K\beta_{1,3}L^0M^r$ lines

Marek Polasik

Faculty of Chemistry, Nicolas Copernicus University, 87-100 Toruń, Poland

(Received 9 February 1995)

Very extensive multiconfiguration-Dirac-Fock calculations in the modified special average-level version with the inclusion of the transverse (Breit) interaction and quantum electrodynamics corrections have been carried out on molybdenum, palladium, and lanthanum to elucidate the structure of the $K\beta_{1,3}L^0M^r$ lines in their x-ray spectra and to explain reliably the influence of additional holes in the M shell on the shapes and positions of $K\beta_{1,3}L^0$ bands. For each type of line, two theoretical spectra have been synthesized, one being a sum of the Lorentzian natural line shapes and the other one being a convolution of the sum of the Lorentzian natural line shapes with the Gaussian instrumental response. It has been shown that the structures of the appropriate groups of $K\beta_{1,3}L^0M^r$ lines of molybdenum, palladium, and lanthanum are similar, while the relevant bands being the sum of the Lorentzian natural line shapes are much smoother for lanthanum (large natural line width) than for molybdenum and palladium. For atoms having sufficiently large atomic numbers (such as lanthanum), the convolution of a sum of the Lorentzian line shapes with the Gaussian instrumental response can be well represented as two Voigt functions in all cases (large distance between the $K\beta_{1,3}L^0M^r$ and $K\beta_{3,3}L^0M^r$ lines). For mid- Z atoms (such as molybdenum and palladium), only in some cases do the resultant bands retain the structure of the reference $K\beta_{1,3}L^0M^0$ lines. It has been found that the most significant effect in producing $K\beta_{1,3}L^0$ energy shifts is the effect of removing a $3s$ electron and, next, a $3p$ electron, while this occurs far less with $3d$ electrons. The shift effects are nonadditive and increase remarkably with increasing atomic number. The results of this and previous papers of this series can be used to determine the M -shell ionization probability in near-central collision processes via the theoretical analysis of various experimental $K\alpha$ and $K\beta$ spectra of molybdenum, palladium, and lanthanum induced by different energetic light ions (such as electron, proton, and He ions) and heavy ions (such as N, O, Ne, Ar, and other ions).

PACS number(s): 32.30.Rj, 32.70.Jz, 31.15.-p

I. INTRODUCTION

Study of the collision processes has always played an important role in the development of modern atomic physics. At the fundamental level it provides data necessary for an evaluation of quantum mechanical models of many-body interactions. At a more practical level the experimental data are of great importance to other branches of physics such as solid state physics, trace element analysis, laser physics, astrophysics, plasma physics, and nuclear physics. In the latter, for example, the analysis of $K\alpha$ and $K\beta$ x-ray spectra of products of nuclear fusion reactions (half-trajectory collisions), which are the result of the inner-shell ionization by projectile, may provide a clock for nuclear reaction studies and valuable insight into the nuclear reaction mechanism [1,2].

In the last two decades, a great deal of attention has been devoted to the understanding of the inner-shell ionization mechanism in collision processes. About 15 years ago, a method was developed to determine L -shell ionization probability in near-central collisions from measured K x-ray spectra of multiply ionized atoms. In the beginning this method was applied to many studies of target atoms with $Z < 30$ [3-24], but since 1987 it has been applied to studies of target atoms with $Z > 40$ [25-31]. Carlen and co-workers [32,33] have extended

this method to determine M -shell ionization probability in near-central collisions with light ions as projectiles.

In the case of the near-central collisions of energetic heavy ions (such as N, O, Ne, and Ar ions) with mid- Z target atoms, multiple ionization of the M and L shells of the target atoms (with simultaneous K -shell ionization) is extremely likely to occur, resulting in a very complex structure of the observed $K\alpha$ and $K\beta$ x-ray spectra. In this case, from the relative intensities of the $K\alpha L^n$ (or $K\beta L^n$) satellite bands (n indicate number of holes in the L shell), which can be resolved in high-resolution spectrometers, we can get the distribution of holes in the L shell at the moment of the x-ray transitions. The primary L -hole distribution at the moment of a collision with a heavy ion can be deduced via statistical scaling procedure, taking into account the competition of other possible decay processes [26]. On the other hand, additional M -shell holes merely broaden and shift the measured lines and it is not possible to deduce the degree of M -shell ionization on the basis of the experimental data only. Therefore, a correct analysis of the K x-ray spectra accompanying the ionization of target atoms in collisions with energetic heavy ions requires theoretical knowledge of the structure of the $K\alpha L^n M^r$ and $K\beta L^n M^r$ lines. Generally, the groups of lines labeled $K\alpha L^n M^r$ and $K\beta L^n M^r$ correspond to transitions from initial states that have one hole in the K shell, n holes in

the L shell, and r holes in the M shell. The $K\beta_{1,3}L^0M^0$ reference lines are usually denoted $1s^{-1} \rightarrow 3p^{-1}$.

In recent years, the author has started to develop and apply theoretical models for reliable descriptions of very complex x-ray spectra of multiply ionized atoms being observed as a result of the ionization processes of target atoms in near-central collisions with energetic heavy ions. In the first study concerning the x-ray spectra of multiply ionized atoms [34], multiconfiguration-Dirac-Fock (MCDF) calculations in average-level (AL) versions with the inclusion of the transverse (Breit) interaction, self-energy, and vacuum polarization corrections have been carried out on palladium to elucidate the structure of the $K\alpha_{1,2}L^nM^0$ satellite lines in its x-ray spectra. The availability of the measured high-resolution x-ray spectra of molybdenum [25] provided the inspiration to perform a theoretical simulation of these spectra, applying a model in which a spectrum was represented as a sum of the bands (which is the convolution of the sum of the Lorentzian natural line shapes with the Gaussian instrumental response) resulting from the transitions of the $K\alpha_{1,2}L^nM^0$ type only [35]. The effect of M -shell holes has been taken into account in a crude way by simply shifting a spectrum towards higher energies and applying larger Gaussian linewidths. Although this procedure has succeeded in general, it has turned out that to reproduce accurately both the positions of the bands and the shape of the experimental spectrum including $K\alpha_{1,2}L^n$ satellite bands it is necessary to perform a detailed investigation in which various M -shell holes are taken into account together with L -shell holes (the $K\alpha_{1,2}L^nM^r$ lines).

In the third and fourth papers of this series, the MCDF method has been successfully applied in an extensive and detailed study of the structure of the $K\alpha_{1,2}L^0M^r$ lines in molybdenum ($Z = 42$), palladium ($Z = 46$), and holmium ($Z = 67$) [36], and also of the structure of the $K\alpha_{1,2}L^1M^r$ lines in palladium [37].

Recently we proposed a method for the analysis of very complex K x-ray spectra accompanying the ionization of the target atoms in near-central collisions with energetic heavy ions [38]. In this method the measured $K\alpha$ and $K\beta$ spectra are simultaneously decomposed into the theoretically constructed line shapes for $K\alpha_{1,2}L^0M^r$ and $K\beta_{1,3}L^0M^r$ transitions, assuming a binomial distribution of holes in the M shell and treating the M -shell ionization probabilities per electron (p_M) as adjustable parameters. Thus, the value of the single p_M parameter is extracted from the best fit of the theoretical profiles to the analyzed spectrum. This is the only known way to extract the p_M from complex K x-ray spectra induced by heavy ions.

To the best of my knowledge, no systematic study has been carried out of the structure of the $K\beta$ lines in the x-ray spectra of heavy elements. Therefore, in this paper I concentrate on the systematic theoretical study of the structure of $K\beta_{1,3}L^0M^r$ lines. To explain reliably the influence of additional holes in the M shell on the shapes and positions of $K\beta_{1,3}L^0$ bands, extensive MCDF studies on the structures of $K\beta_{1,3}L^0M^r$ lines have been performed for molybdenum, palladium, and lanthanum in the modified special average-level (MCDF-MSAL) ver-

sion (see Sec. II) with the inclusion of the transverse (Breit) interaction, self-energy, and vacuum polarization corrections.

The results of these as well as previous studies were implemented in theoretical analyses of $K\alpha_{1,2}L^0M^r$ and $K\beta_{1,3}L^0M^r$ x-ray spectra of molybdenum [38] and of palladium and lanthanum [39] generated in near-central collisions of the above-mentioned atoms with oxygen ions and have potential application in theoretical analyses of various experimental x-ray spectra induced by collisions with helium, nitrogen, neon, argon, and other ions. It is worth noting that the calculations performed for one specific target atom are sufficient to describe its ionization in a collision with incident ions having a wide range of Z numbers.

II. MCDF CALCULATIONS

The MCDF method used in the present study has been described in detail in many papers [42–47,38]. Therefore, only a brief description will be given here pointing out the essential details. Within the MCDF scheme, the effective Hamiltonian for an N -electron system is to be expressed by

$$H = \sum_{i=1}^N h_D(i) + \sum_{j>i=1}^N C_{ij}, \quad (1)$$

where $h_D(i)$ is the Dirac operator for i th electron and the terms C_{ij} account for electron-electron interactions and come from the one-photon exchange process. The latter are a sum of the Coulomb interaction operator (due to longitudinally polarized photons) and the transverse Breit operator (due to transversely polarized photons).

In the MCDF method an atomic state function with total angular momentum J and parity p is assumed in the multiconfigurational form

$$\Psi_s(J^p) = \sum_m c_m(s) \Phi(\gamma_m J^p), \quad (2)$$

where $\Phi(\gamma_m J^p)$ are configuration state functions (CSF), $c_m(s)$ are the configuration mixing coefficients for state s , and γ_m represents all information required to uniquely define a certain CSF.

Various versions of MCDF calculations can be defined by the choice of the form of the energy functional. In the standard optimal-level version of MCDF (MCDF-OL) calculations we get for a particular state the optimal energy, the optimal set of one-electron spinors, and the optimal set of the CSF mixing coefficients $\{c_m(s)\}$. The application of the MCDF-OL version to the calculations of the transition probabilities should take into account the fact of nonorthogonality of the spinors corresponding to the pairs of initial and final states. Moreover, in the theoretical studies on x-ray transitions, we must not forget that for many cases they occur between hundreds of states. The application of the MCDF-OL method for those studies would thus imply a separate MCDF-OL

calculation for each state, which is very time consuming.

In order to cope with the above difficulties, some other methods (different from MCDF-OL) are used to study the transition probabilities. The main feature of those methods is the fact that they use a common set of orbitals for all initial and final states. Two standard schemes have been elaborated up to the present which are based on this idea, namely, the average-level version of MCDF (MCDF-AL) and extended average-level version of MCDF (MCDF-EAL).

Preliminary test calculations have shown that MCDF-AL and MCDF-EAL schemes are indeed not accurate enough in some cases. The reason for the insufficient accuracy of the MCDF-AL (or MCDF-EAL) approach seems to be the fact that the functional does not consider the different number of initial and final states. Therefore, the orbitals obtained in this scheme in a sense favor those states (initial or final) that are more numerous. Because the essence of the present investigations is the reliable calculations of the transition energies and transition probabilities between the initial and final states, it is appropriate to formulate a functional that compensates to some extent for this imbalance.

Therefore, in the modified special average-level version of MCDF calculations, which is used in this work, the energy functional can be expressed by

$$E = E_{opt} \sum_a \bar{q}_a \epsilon_a S(a, a) + \sum_{\substack{a,b \\ a \neq b}} \epsilon_{a,b} S(a, b), \quad (3)$$

where \bar{q}_a is the generalized occupation number for the orbital a , ϵ_a and ϵ_{ab} are the Lagrange multipliers, $S(a, b)$ is the overlap integral, and E_{opt} [38] is taken in the form

$$E_{opt} = \frac{1}{\lambda + 1} \left[\frac{\lambda}{n_i} \sum_{i=1}^{n_i} H_{ii} + \frac{1}{n_f} \sum_{f=1}^{n_f} H_{ff} \right], \quad (4)$$

where H_{ii} and H_{ff} are the diagonal contributions to the Hamiltonian matrix, the first sum runs over all the initial CSFs (n_i), and the second sum runs over all the final CSFs (n_f). The presence of a factor λ in formula (4) compensates in a simple way for the difference in quality of descriptions of initial and final states, which is the

main problem in performing reliable theoretical (MCDF) studies of the structure of $K\alpha_{1,2}L^nM^r$, $K\beta_{1,3}L^nM^r$, and $K\beta_2L^nM^r$ lines in the x-ray spectra.

One can see that if λ is equal to 1 we will obtain a formula in which exaggerating the contribution of the more numerous states (initial or final) to the energy functional is completely compensated. This results in a good reproduction of the relative positions of the spectral lines. However, for $\lambda = 1$ the calculated (diagram and satellite) transition energies are shifted for the type of transition considered (such as $K\alpha_{1,2}L^nM^r$, $K\beta_{1,3}L^nM^r$, and $K\beta_2L^nM^r$) by similar amounts relative to experimental ones. Test calculations have shown that the optimum values of λ depend strongly on the type of spectral line, but is almost independent of atom type. They can therefore be treated as a parameter characteristic of the type of spectral line. It is very significant that this simple formula, with the particular values of $\lambda = 0.5, 0.65$, and 0.8 for $K\alpha_{1,2}L^nM^r$, $K\beta_{1,3}L^nM^r$, and $K\beta_2L^nM^r$ transitions, respectively, reproduces very well experimental diagram (see Table I and Refs. [33,38,39]) and satellite (see Ref. [33]) lines for medium Z atoms. Therefore, formula (4) provides a simple and effective way of calculating the absolute positions of spectral lines.

This functional has already been applied with success in the extensive MCDF study on the structure of $K\alpha_{1,2}L^nM^r$ and $K\beta_{1,3}L^nM^r$ lines in the x-ray spectra induced in near-central collisions of the oxygen ions with molybdenum [38], and with palladium and lanthanum [39]. Recently, it has been used in the study of the $K\alpha_{1,2}L^nM^r$, $K\beta_{1,3}L^nM^r$, and $K\beta_2L^nM^r$ lines in zirconium, molybdenum, palladium, and praseodymium [40] generated by helium ions and also $K\beta_2L^nM^r$ lines in zirconium, molybdenum, and palladium induced by proton and photon beams [41]. The present studies are based on the GRASP (general-purpose relativistic atomic structure program) package [47], which allows relativistic MCDF calculations with the inclusion of the transverse (Breit) interaction and QED (self-energy and vacuum polarization) corrections.

III. RESULTS AND DISCUSSION

As pointed out in the Introduction, accurate analysis of the K x-ray spectra accompanying the ionization of tar-

TABLE I. Comparison of the theoretical $K\alpha L^0 M^0$ and $K\beta L^0 M^0$ transition energies (E_{theor}) calculated in the MCDF-MSAL scheme for molybdenum, palladium, and lanthanum with their experimental (E_{expt}) counterparts [48].

| Transition type | Energy (in eV) | | | | | |
|---------------------|----------------|------------|-------------|------------|-------------|------------|
| | Mo | | Pd | | La | |
| | E_{theor} | E_{expt} | E_{theor} | E_{expt} | E_{theor} | E_{expt} |
| $K\alpha_2 L^0 M^0$ | 17374.8 | 17374.3(1) | 21020.3 | 21020.1(1) | 33033.2 | 33034.1(2) |
| $K\alpha_1 L^0 M^0$ | 17479.6 | 17479.3(2) | 21177.1 | 21177.1(1) | 33440.4 | 33441.8(2) |
| $K\beta_3 L^0 M^0$ | 19589.8 | 19590.3(3) | 23791.4 | 23791.1(2) | 37718.0 | 37720.2(5) |
| $K\beta_1 L^0 M^0$ | 19607.4 | 19608.3(3) | 23819.2 | 23818.7(2) | 37798.6 | 37801.0(3) |

get atoms in collisions with energetic heavy ions requires theoretical knowledge of the structure of the $K\alpha L^0 M^r$ and $K\beta L^0 M^r$ lines. To explain reliably the influence of various types of additional holes in the M shell on the shapes and positions of $K\beta_{1,3}L^0$ bands, extensive MCDF studies on the structure of $K\beta_{1,3}L^0 M^r$ lines have been performed for molybdenum, palladium, and lanthanum in the modified average-level version (see Sec. II).

The usability of the MCDF method with the inclusion of the transverse (Breit) interaction, self-energy, and vacuum polarization corrections in the studies of the structures of x-ray lines is well known [34,37]. To test the quality of the MCDF-MSAL scheme used in further studies, I first compared the calculated $K\alpha_{1,2}L^0 M^0$ and $K\beta_{1,3}L^0 M^0$ transition energies for molybdenum, palladium, and lanthanum with their experimental counterparts (see Table I). For each $K\alpha_{1,2}L^0 M^0$ and $K\beta_{1,3}L^0 M^0$ transition the MCDF-MSAL results were in excellent agreement with experiment. This means that the MCDF-MSAL scheme is adequate to describe reliably the relevant states and reproduce correctly the effect of removing M -shell electrons on the $K\beta_{1,3}L^0$ bands.

Let us consider the “pure” $K\beta_{1,3}L^0 M^r$ transitions, i.e., those in which there are no holes in shells higher than M . All types of transitions considered here can be classified into groups, depending on the number of holes in the M shell in the initial states. These are $K\beta_{1,3}L^0 M^0$ (reference lines), $K\beta_{1,3}L^0 M^1$ (preliminary results for Mo have been presented in Ref. [38]), and $K\beta_{1,3}L^0 M^2$.

In Figs. 1–6, both stick and synthesized spectra for all types of $K\beta_{1,3}L^0 M^r$ transitions ($r = 0, 1, \text{ and } 2$) for molybdenum, palladium, and lanthanum are presented, together with the summary spectra for a particular r . Two synthesized spectra for all cases have been constructed, one being the sum of the Lorentzian natural line shapes with a width of 6.5 eV for Mo, 8.5 eV for Pd, and 19.5 eV for La [49] (dotted lines) and, to better simulate the experimental spectra, the other one (solid lines) being a convolution of the sum of the Lorentzian natural line shapes with the Gaussian instrumental response having a width of 8.0 eV for Mo [38], 11.0 eV for Pd, and 32.0 eV for La [39].

For the simplest case of the $K\beta_{1,3}L^0 M^r$ transitions ($K\beta_{1,3}L^0 M^0$ reference lines) for all atoms, two well resolved lines are present, namely, $K\beta_1 L^0 M^0$ and $K\beta_3 L^0 M^0$ [see Figs. 1(a), 2(a), and 3(a)]. It is worth noting that the distance between the $K\beta_1 L^0 M^0$ and $K\beta_3 L^0 M^0$ lines strongly increases with Z . The separation is 18.0 eV, 27.6 eV, and 80.8 eV for Mo ($Z = 42$), Pd ($Z = 46$), and La ($Z = 57$), respectively.

In the case of $K\beta_{1,3}L^0 M^1$ lines (see Figs. 1–3) we have three possible types of transitions: $(1s3s)^{-1} \rightarrow (3s3p)^{-1}$, $(1s3p)^{-1} \rightarrow 3p^{-2}$, and $(1s3d)^{-1} \rightarrow (3p3d)^{-1}$. In the first case there are 6 states and 6 possible transitions, while in the second case there are 9 states and 14 transitions, of which 11 are of a remarkable intensity. In the last transition type there are 16 states and 36 transitions, of which 34 are of a remarkable intensity. In this case the distances between the neighboring lines are small. It can be noted (see the stick spectra in Figs. 1–3) that the structures of the appropriate groups of $K\beta_{1,3}L^0 M^r$ lines of

molybdenum, palladium, and lanthanum are similar. For all types of $K\beta_{1,3}L^0 M^r$ transitions, weakly structured bands (much smoother for lanthanum than for molybdenum and palladium) are observed only in the case of a sum of Lorentzian line shapes (dotted lines), while the convolution of Lorentzian line shapes with Gaussian instrumental response greatly smooths the resultant spectra. For lanthanum, the resultant spectra (solid lines) retain the structure of the reference lines $K\beta_{1,3}L^0 M^0$ in all cases (large distance between the $K\beta_1 L^0 M^r$ and $K\beta_3 L^0 M^r$ lines), while for molybdenum and palladium this occurs only in the case of $(1s3p)^{-1} \rightarrow 3p^{-2}$ transitions.

In the case of $K\beta_{1,3}L^0 M^2$ we have six possible types of transitions: $1s^{-1}3s^{-2} \rightarrow 3s^{-2}3p^{-1}$, $1s^{-1}3p^{-2} \rightarrow 3p^{-3}$, $1s^{-1}3d^{-2} \rightarrow 3p^{-1}3d^{-2}$, $(1s3s3p)^{-1} \rightarrow 3s^{-1}3p^{-2}$, $(1s3s3d)^{-1} \rightarrow (3s3p3d)^{-1}$, and $(1s3p3d)^{-1} \rightarrow 3p^{-2}3d^{-1}$. Both stick and synthesized theoretical spectra are displayed in Figs. 4, 5, and 6 for molybdenum, palladium, and lanthanum, respectively. The first one is the sim-

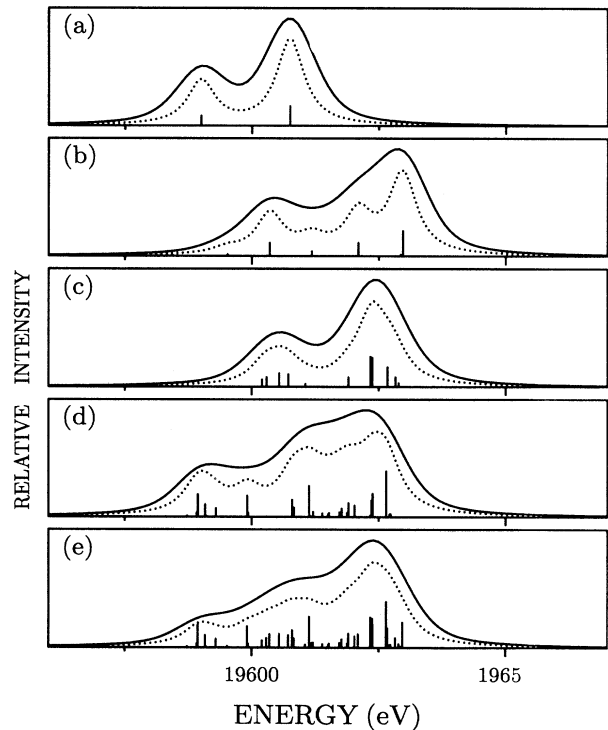


FIG. 1. Calculated stick (line positions with their relative intensities) and synthesized [one being the sum of the Lorentzian natural line shapes (dotted lines) and the other obtained by convolution of the sum of the Lorentzian natural line shapes with the Gaussian instrumental response (solid lines)] for $K\beta_{1,3}L^0 M^0$ and $K\beta_{1,3}L^0 M^1$ transitions in molybdenum of the types (a) $1s^{-1} \rightarrow 3p^{-1}$ ($K\beta_{1,3}L^0 M^0$ reference lines), (b) $(1s3s)^{-1} \rightarrow (3s3p)^{-1}$, (c) $(1s3p)^{-1} \rightarrow 3p^{-2}$, (d) $(1s3d)^{-1} \rightarrow (3p3d)^{-1}$, and (e) for $K\beta_{1,3}L^0 M^1$ —summary spectrum [(a)–(d)].

TABLE II. Number of transitions for each transition type and the theoretical relative average positions of each group of $K\beta_{1,3}L^0M^r$ lines (with respect to $K\beta_{1,3}L^0M^0$) for molybdenum, palladium, and lanthanum.

| Transition type | The number of transitions | Energy shifts (eV) | | |
|---|---------------------------|--------------------|------|------|
| | | Mo | Pd | La |
| $1s^{-1} \rightarrow 3p^{-1}$ | 2 | 0.0 | 0.0 | 0.0 |
| $(1s3s)^{-1} \rightarrow (3s3p)^{-1}$ | 6 | 17.8 | 20.4 | 31.0 |
| $(1s3p)^{-1} \rightarrow 3p^{-2}$ | 14 | 16.8 | 19.5 | 30.1 |
| $(1s3d)^{-1} \rightarrow (3p3d)^{-1}$ | 36 | 10.5 | 12.5 | 20.8 |
| $K\beta_{1,3}L^0M^1$ | 56 | 13.2 | 15.5 | 24.7 |
| $1s^{-1}3s^{-2} \rightarrow 3s^{-2}3p^{-1}$ | 2 | 36.5 | 41.4 | 62.7 |
| $1s^{-1}3p^{-2} \rightarrow 3p^{-3}$ | 35 | 34.4 | 39.5 | 60.9 |
| $1s^{-1}3d^{-2} \rightarrow 3p^{-1}3d^{-2}$ | 401 | 21.9 | 25.7 | 42.4 |
| $(1s3s3p)^{-1} \rightarrow 3s^{-1}3p^{-2}$ | 47 | 35.4 | 40.4 | 61.8 |
| $(1s3s3d)^{-1} \rightarrow (3s3p3d)^{-1}$ | 131 | 29.1 | 33.5 | 52.5 |
| $(1s3p3d)^{-1} \rightarrow 3p^{-2}3d^{-1}$ | 413 | 28.1 | 32.6 | 51.6 |
| $K\beta_{1,3}L^0M^2$ | 1029 | 27.3 | 31.6 | 50.1 |

plest case as far as the $K\beta_{1,3}L^0M^r$ lines are concerned because its structure is identical to the structure of the $K\beta_{1,3}L^0M^0$ reference lines. In the remaining cases the number of transitions is very great (see Table II). In some cases [e.g., $1s^{-1}3d^{-2} \rightarrow 3p^{-1}3d^{-2}$ and $(1s3p3d)^{-1} \rightarrow 3p^{-2}3d^{-1}$] it can be observed that the structure of the spectra is very complex (more than 400 transitions) and

the distances between the neighboring lines become extremely small. Moreover, the structures of the appropriate groups of $K\beta_{1,3}L^0M^r$ lines of molybdenum, palladium, and lanthanum are similar (see stick spectra in Figs. 4–6) while the relevant $K\beta_{1,3}L^0M^r$ bands that are the sum of the Lorentzian natural line shapes are much smoother for lanthanum than for molybdenum and pal-

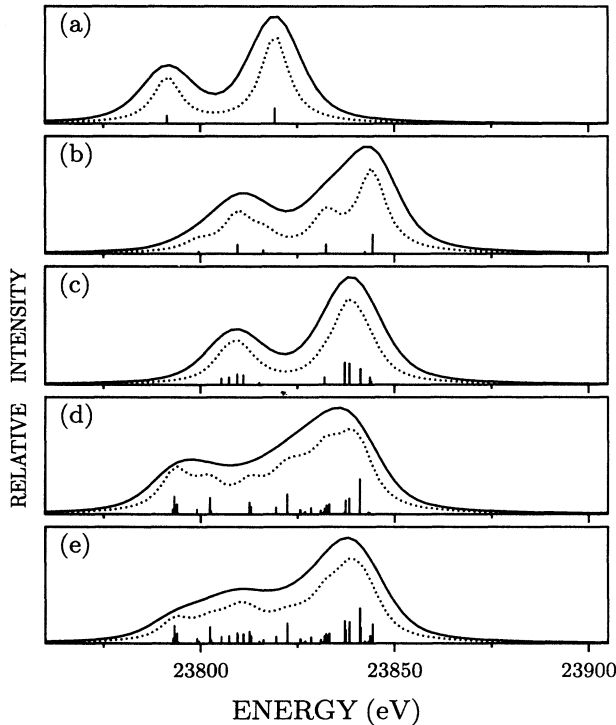


FIG. 2. Same as Fig. 1, but for $K\beta_{1,3}L^0M^0$ and $K\beta_{1,3}L^0M^1$ transitions in palladium.

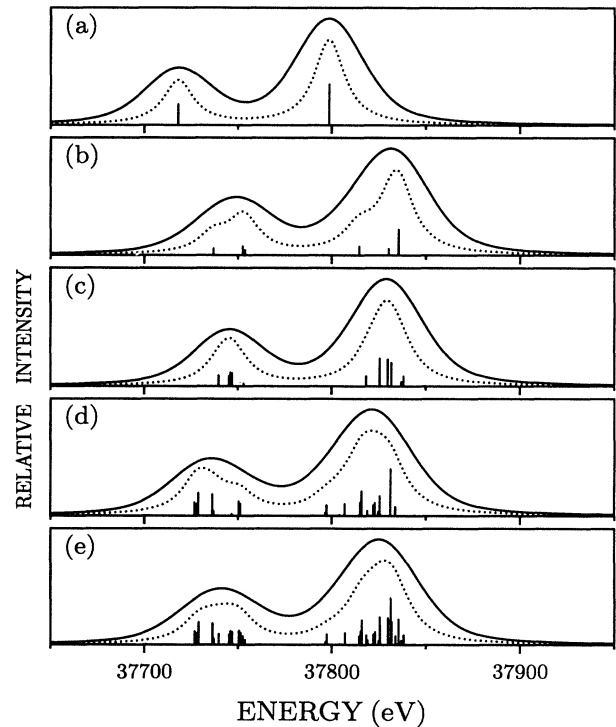


FIG. 3. Same as Fig. 1, but for $K\beta_{1,3}L^0M^0$ and $K\beta_{1,3}L^0M^1$ transitions in lanthanum.

ladium.

Generally, it can be seen that in most cases, removing even one or two electrons from the M shell causes a strong increase in the number of possible transitions. It can be found that for all types of the $K\beta_{1,3}L^0M^r$ transitions [with the exception of $1s^{-1}3s^{-2} \rightarrow 3s^{-2}3p^{-1}$ and $(1s3s)^{-1} \rightarrow (3s3p)^{-1}$] the distances between the neighboring lines are very small, i.e., of the order of 0.1–5 eV for palladium.

It can be noted for molybdenum and palladium that the theoretically synthesized spectrum that is the sum of the Lorentzian natural line shapes (dotted lines) has

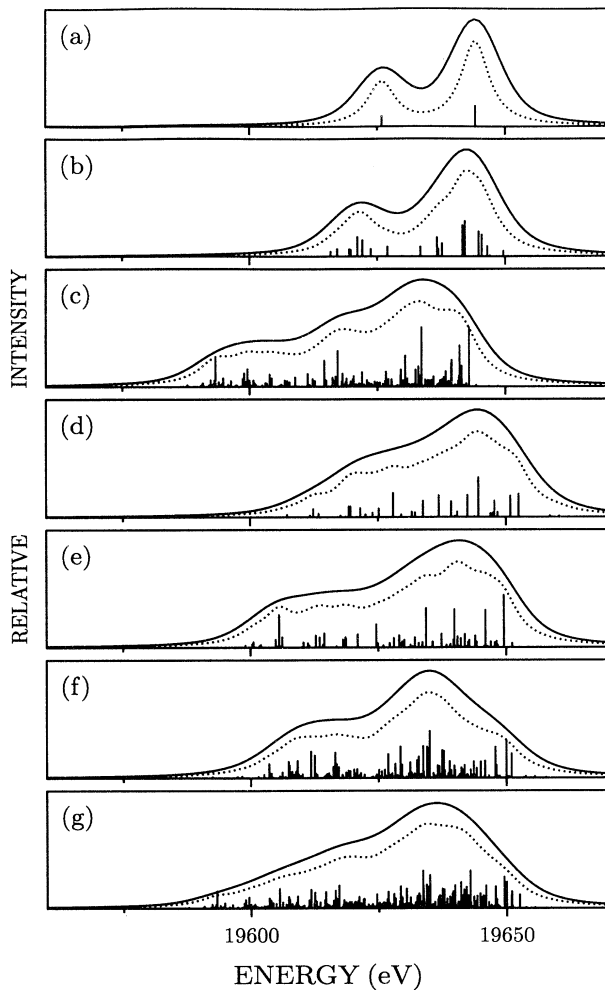


FIG. 4. Calculated stick and synthesized spectra [the sum of the Lorentzian components (dotted lines) and the convolution of the sum of the Lorentzian natural line shapes with the Gaussian instrumental response (solid lines)] for $K\beta_{1,3}L^0M^2$ transitions in molybdenum of the types (a) $1s^{-1}3s^{-2} \rightarrow 3s^{-2}3p^{-1}$, (b) $1s^{-1}3p^{-2} \rightarrow 3p^{-3}$, (c) $1s^{-1}3d^{-2} \rightarrow 3p^{-1}3d^{-2}$, (d) $(1s3s3p)^{-1} \rightarrow 3s^{-1}3p^{-2}$, (e) $(1s3s3d)^{-1} \rightarrow (3s3p3d)^{-1}$, (f) $(1s3p3d)^{-1} \rightarrow 3p^{-2}3d^{-1}$, and (g) for $K\beta_{1,3}L^0M^2$ —summary spectrum [(a)–(f)].

a subtle structure that is substantially lost after convolution with the Gaussian instrumental response (solid lines). Moreover, for all types of the $K\beta_{1,3}L^0M^r$ transitions of molybdenum and palladium [with the exception of $(1s3p)^{-1} \rightarrow 3p^{-2}$, $1s^{-1}3s^{-2} \rightarrow 3s^{-2}3p^{-1}$, and $1s^{-1}3p^{-2} \rightarrow 3p^{-3}$] the resultant bands have the form of one shapeless and broad peak and cannot be well represented as the sum of two Voigt functions. In the case of lanthanum (see Figs. 3 and 6), only for a sum of Lorentzian line shapes are very weakly structured bands ($K\beta_1L^0M^r$ and $K\beta_3L^0M^r$) observed, while for the convolution of the sum of the Lorentzian line shapes with the Gaussian instrumental response, the shapes of both bands are very smooth. Moreover, for lanthanum two clearly separated groups of lines ($K\beta_1L^0M^r$ and $K\beta_3L^0M^r$) are observed for each type of transition and the resultant bands can be well represented as two Voigt functions.

A comparison of Figs. 1–3 and Figs. 4–6 indicates that

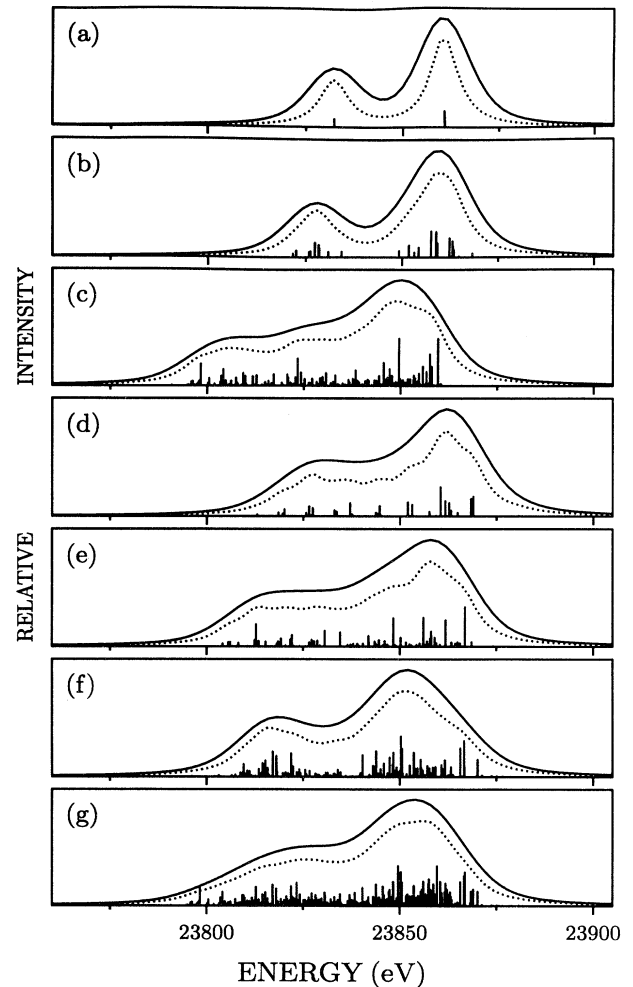


FIG. 5. Same as Fig. 4, but for $K\beta_{1,3}L^0M^2$ transitions in palladium.

the structures of the appropriate groups of $K\beta_{1,3}L^0M^r$ lines of molybdenum, palladium, and lanthanum are similar (see stick spectra), while the relevant bands that are the sum of the Lorentzian natural line shapes (see dotted lines) are much smoother for lanthanum than for molybdenum and palladium. For lanthanum the convolution of the sum of the Lorentzian line shapes with the Gaussian instrumental response (see solid lines) retains the structure of the reference lines $K\beta_{1,3}L^0M^0$ in all cases (large distance between the $K\beta_1L^0M^r$ and $K\beta_3L^0M^r$ lines), while for molybdenum and palladium this occurs only in the case of $(1s3p)^{-1} \rightarrow 3p^{-2}$, $1s^{-1}3s^{-2} \rightarrow 3s^{-2}3p^{-1}$ (the effect of removing the whole $3s$ subshell), and $1s^{-1}3p^{-2} \rightarrow 3p^{-3}$ transitions. It can be seen that for all cases (with the exception of $1s^{-1}3s^{-2} \rightarrow 3s^{-2}3p^{-1}$) the widths of $K\beta_{1,3}L^0M^r$ bands obtained by the convolution of a sum of the Lorentzian line shapes with the Gaussian instrumental response are greater than the widths of reference $K\beta_{1,3}L^0M^0$ bands. It can also be found

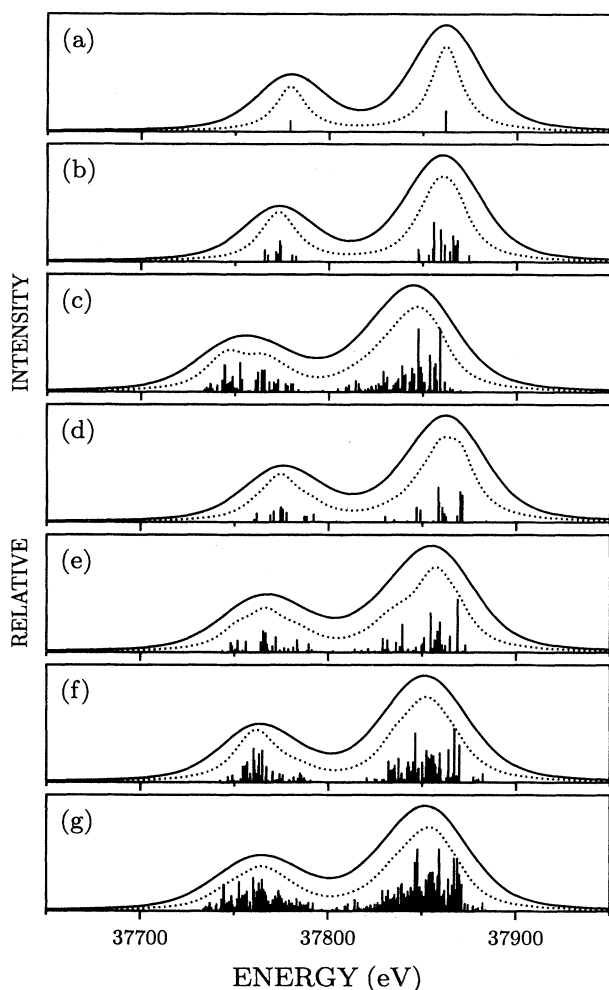


FIG. 6. Same as Fig. 4, but for $K\beta_{1,3}L^0M^2$ transitions in lanthanum.

that because the positions of various types of $K\beta_{1,3}L^0M^r$ bands are shifted by a different amount (with respect to $K\beta_{1,3}L^0M^0$), the summary $K\beta_{1,3}L^0M^r$ spectra for certain r are broader (and smoother) than the particular components.

The theoretical relative “average” positions of each group of $K\beta_{1,3}L^0M^r$ lines (with respect to $K\beta_{1,3}L^0M^0$) for molybdenum, palladium, and lanthanum have been given in Table II. It can be found from Table II that removing a $3s$ electron is more effective in producing the $K\beta L^0$ energy shift (towards higher energies) than removing a $3p$ electron and much more than removing a $3d$ electron. It can also be observed that the shift effects are strongly nonadditive and increase remarkably with the atomic number.

Only the structures of the particular types of groups of $K\beta_{1,3}L^0M^r$ lines and the summary spectra of all types (for certain r) have been presented above. In fact, the situation is much more complex, because the real $K\beta_{1,3}L^0M$ bands consist, in general, of all the groups of lines (corresponding to all the possible $K\beta_{1,3}L^0M^r$ transitions) which also strongly overlap. Therefore, to simulate theoretically the bands that are experimentally observed as the “ $K\beta_{1,3}L^0$ ” bands one should combine linearly all contributions to the $K\beta_{1,3}L^0M^r$ type spectrum.

IV. CONCLUSIONS

The test studies have shown that the MCDF-MSAL version of the MCDF method with the inclusion of the transverse (Breit) interaction, self-energy, and vacuum polarization corrections is accurate enough to describe reliably the relevant states and reproduce correctly the effect of removing M -shell electrons on the $K\beta_{1,3}L^0$ bands.

To explain reliably the influence of additional holes in the M shell on the shapes and positions of $K\beta_{1,3}L^0$ bands, considerable attention has been paid to the analysis of the structure of the groups of $K\beta_{1,3}L^0M^r$ lines corresponding to various types of transitions. On the basis of the calculations for molybdenum, palladium, and lanthanum, some general conclusions can be drawn.

First, in the case of $K\beta_{1,3}L^0M^0$ reference lines for all atoms, two well-resolved lines are observed, namely, $K\beta_1L^0M^0$ and $K\beta_3L^0M^0$. It is worth noting that the distance between the $K\beta_1L^0M^0$ and $K\beta_3L^0M^0$ lines strongly increases with Z . Second, in most cases, removing even a small number of electrons from the M shell causes a strong increase in the number of states possible for the given initial and final configurations and a dramatic increase in the number of possible transitions. In some cases, the structures of the $K\beta_{1,3}L^0M^r$ lines are very complex and the distances between the neighboring lines are very small, i.e., of the order of 0.1–5.0 eV for palladium. Third, the structures of the appropriate groups of $K\beta_{1,3}L^0M^r$ lines of molybdenum, palladium, and lanthanum are similar, while the relevant bands that are the sum of the Lorentzian natural line shapes are much smoother for lanthanum (large natural line width) than for molybdenum and palladium. Fourth, for atoms having sufficiently large atomic numbers (such as lan-

thanum), the convolution of a sum of the Lorentzian line shapes with the Gaussian instrumental response retains the structure of the reference lines $K\beta_{1,3}L^0M^0$ in all cases (large distance between the $K\beta_1L^0M^r$ and $K\beta_3L^0M^r$ lines) and the resultant bands can be well represented as two Voigt functions. For mid- Z atoms (such as molybdenum and palladium) only in the case of $(1s3p)^{-1} \rightarrow 3p^{-2}$, $1s^{-1}3s^{-2} \rightarrow 3s^{-2}3p^{-1}$ (the effect of removing the whole $3s$ subshell) and $1s^{-1}3p^{-2} \rightarrow 3p^{-3}$ transitions do the resultant bands retain the structure of the reference lines $K\beta_{1,3}L^0M^0$. Fifth, for all cases (with the exception of $1s^{-1}3s^{-2} \rightarrow 3s^{-2}3p^{-1}$) the widths of the $K\beta_{1,3}L^0M^r$ bands are significantly greater than the widths of reference $K\beta_{1,3}L^0M^0$ bands. Because the positions of various types of $K\beta_{1,3}L^0M^r$ bands are shifted by a different amount, the summary $K\beta_{1,3}L^0M^r$ spectra for certain r are broader (and smoother) than the particular components. Because the $K\beta_{1,3}L^0M^r$ bands corresponding to various r are strongly overlapped, the effects of multiple M -shell ionization are manifested in the spectra as an asymmetric broadening and a net shift of $K\beta_{1,3}L^0$ bands. Sixth, the most significant effect in producing $K\beta_{1,3}L^0$ energy shifts is the effect of removing a $3s$ electron and next a $3p$ electron, while this occurs far less with $3d$ electrons. The shift effects are strongly non-additive and increase remarkably with increasing atomic number.

The author believes that the results of his analysis will be helpful in achieving better understanding of the structure of the $K\beta_{1,3}L^0M^r$ lines in x-ray spectra of multiply ionized heavy atoms. Moreover, the results of this work can be used to construct different shape theoretical $K\beta_{1,3}L^0$ bands for molybdenum, palladium, and lanthanum, satisfactorily reproducing the shapes of various experimental $K\beta_{1,3}L^0$ bands generated by different energetic light ions (such as electron, protons, and helium ions) and heavy ions (such as nitrogen, oxygen, neon, argon, and other ions).

Obviously, the present study concerns the effect of M -shell holes on the principal $K\beta_{1,3}L^0$ bands only. Undoubtedly, for a complete description of the heavy-particles-induced x-ray spectra, it is necessary to perform calculations on all the possible $K\beta_{1,3}L^rM^r$ transitions and to examine the effect of N -shell holes. Investigations are already in progress and the results will be published in forthcoming papers. Also, both theoretical and experimental research with other target atoms has been initiated and the results will be reported soon.

ACKNOWLEDGMENT

This work was supported by the Polish Committee for Scientific Research (KBN), Grant No. 223229203.

- [1] Z. Sujkowski, D. Chmielewska, P. Rymuza, G. J. Balster, B. Kotlinski, R. H. Siemssen, and H. W. Wilschut, Phys. Lett. B **196**, 122 (1987).
- [2] P. Rymuza, D. Chmielewska, Z. Sujkowski, G. J. Balster, B. Kotlinski, R. H. Siemssen, and H. W. Wilschut, Nucl. Phys. A **517**, 159 (1990).
- [3] P. Richard, I. L. Morgan, T. Furuta, and D. Burch, Phys. Rev. Lett. **23**, 1009 (1969).
- [4] A. R. Knudson, D. J. Nagel, P. G. Burkhalter, and K. L. Dunning, Phys. Rev. Lett. **26**, 1149 (1971).
- [5] D. Burch, P. Richard, and R. L. Blake, Phys. Rev. Lett. **26**, 1355 (1971).
- [6] D. G. McCrary and P. Richard, Phys. Rev. A **5**, 1249 (1972).
- [7] D. G. McCrary, M. Senglaub, and P. Richard, Phys. Rev. A **6**, 263 (1972).
- [8] C. F. Moore, M. Senglaub, B. Johnson, and P. Richard, Phys. Lett. **40A**, 107 (1972).
- [9] P. G. Burkhalter, A. R. Knudson, D. J. Nagel, and K. L. Dunning, Phys. Rev. A **6**, 2093 (1972).
- [10] C. F. Moore, D. K. Olsen, B. Hodge, and P. Richard, Z. Phys. **257**, 288 (1972).
- [11] R. L. Kauffman, J. H. McGuire, P. Richard, and C. F. Moore, Phys. Rev. A **8**, 1233 (1973).
- [12] T. K. Li, R. L. Watson, and J. S. Hansen, Phys. Rev. A **8**, 1258 (1973).
- [13] P. Richard, R. L. Kauffman, J. H. McGuire, C. F. Moore, and D. K. Olson, Phys. Rev. A **8**, 1369 (1973).
- [14] J. McWherter, J. Bolger, C. F. Moore, and P. Richard, Z. Phys. **263**, 283 (1973).
- [15] F. Hopkins, D. O. Elliot, C. P. Bhalla, and P. Richard, Phys. Rev. A **8**, 2952 (1973).
- [16] R. L. Watson, F. E. Jenson, and T. Chiao, Phys. Rev. A **10**, 1230 (1974).
- [17] A. R. Knudson, P. G. Burkhalter, and D. J. Nagel, Phys. Rev. A **10**, 2118 (1974).
- [18] R. L. Kauffman, C. W. Wood, K. A. Jamison, and P. Richard, Phys. Rev. A **11**, 872 (1975).
- [19] K. W. Hill, B. L. Doyle, S. M. Shafroth, D. H. Madison, and R. D. Deslattes, Phys. Rev. A **13**, 1334 (1976).
- [20] J. A. Demarest and R. L. Watson, Phys. Rev. A **17**, 1302 (1978).
- [21] C. Schmiedekamp, B. L. Doyle, T. J. Gray, R. K. Gardner, K. A. Jamison, and P. Richard, Phys. Rev. A **18**, 1892 (1978).
- [22] R. L. Watson, B. I. Sonobe, J. A. Demarest, and A. Langenberg, Phys. Rev. A **19**, 1529 (1979).
- [23] T. Tonuma, Y. Awaya, T. Kambara, H. Kumagai, I. Kohno, and S. Özkök, Phys. Rev. A **20**, 989 (1979).
- [24] R. L. Watson, J. R. White, A. Langenberg, R. A. Kenefick, and C. C. Bahr, Phys. Rev. A **22**, 582 (1980).
- [25] B. Perny, J.-Cl. Dousse, M. Gasser, J. Kern, Ch. Rhême, P. Rymuza, and Z. Sujkowski, Phys. Rev. A **36**, 2120 (1987).
- [26] P. Rymuza, Z. Sujkowski, M. Carlen, J.-Cl. Dousse, M. Gasser, J. Kern, B. Perny, and Ch. Rhême, Z. Phys. D **14**, 37 (1989).
- [27] R. Salziger, G. L. Borchert, D. Gotta, O. W. B. Schult, D. H. Jakubassa-Amundsen, P. A. Amundsen, and K. Rashid, J. Phys. B **22**, 821 (1989).
- [28] D. F. Anagnostopoulos, G. L. Borchert, D. Gotta, and K. Raschid, Z. Phys. D **18**, 139 (1991).
- [29] D. F. Anagnostopoulos, G. L. Borchert, and D. Gotta, J. Phys. B **25**, 2771 (1992).

- [30] P. Rymuza, T. Ludziejewski, Z. Sujkowski, M. Carlen, J.-Cl. Dousse, M. Gasser, J. Kern, and Ch. Rhême, *Z. Phys. D* **23**, 81 (1992).
- [31] T. Ludziejewski, P. Rymuza, Z. Sujkowski, D. Anagnostopoulos, G. Borchert, M. Carlen, J.-Cl. Dousse, J. Hozowska, J. Kern, and Ch. Rhême, *Acta Phys. Polon. B* **25**, 699 (1994).
- [32] M. Carlen, J.-Cl. Dousse, M. Gasser, J. Kern, Ch. Rhême, P. Rymuza, Z. Sujkowski, and D. Trautmann, *Europhys. Lett.* **13**, 231 (1990).
- [33] M. Carlen, J.-Cl. Dousse, M. Gasser, J. Hozowska, J. Kern, Ch. Rhême, P. Rymuza, and Z. Sujkowski, *Z. Phys. D* **23**, 71 (1992).
- [34] M. Polasik, *Phys. Rev. A* **39**, 616 (1989).
- [35] M. Polasik, *Phys. Rev. A* **39**, 5092 (1989).
- [36] M. Polasik, *Phys. Rev. A* **40**, 4361 (1989).
- [37] M. Polasik, *Phys. Rev. A* **41**, 3689 (1990).
- [38] M. W. Carlen, M. Polasik, B. Boschung, J.-Cl. Dousse, M. Gasser, Z. Halabuka, J. Hozowska, J. Kern, B. Perny, Ch. Rhême, P. Rymuza, and Z. Sujkowski, *Phys. Rev. A* **46**, 3893 (1992).
- [39] M. W. Carlen, B. Boschung, J.-Cl. Dousse, M. Gasser, Z. Halabuka, J. Hozowska, J. Kern, B. Perny, Ch. Rhême, M. Polasik, P. Rymuza, and Z. Sujkowski, *Phys. Rev. A* **49**, 2524 (1994).
- [40] B. Boschung, M. W. Carlen, J.-Cl. Dousse, B. Galley, Z. Halabuka, Ch. Herren, J. Hozowska, J. Kern, Ch. Rhême, T. Ludziejewski, M. Polasik, P. Rymuza, and Z. Sujkowski, *PSI Annual Report* (Paul Scherrer Institut, Villigen, 1993), Vol. 147.
- [41] T. Ludziejewski, P. Rymuza, Z. Sujkowski, B. Boschung, J.-Cl. Dousse, B. Galley, Z. Halabuka, Ch. Herren, J. Hozowska, J. Kern, Ch. Rhême, and M. Polasik, *Phys. Rev. A* (to be published).
- [42] I. P. Grant, B. J. McKenzie, P. H. Norrington, D. F. Mayers, and N. C. Pyper, *Comput. Phys. Commun.* **21**, 207 (1980).
- [43] B. J. McKenzie, I. P. Grant, and P. H. Norrington, *Comput. Phys. Commun.* **21**, 233 (1980).
- [44] I. P. Grant and B. J. McKenzie, *J. Phys. B* **13**, 2671 (1980).
- [45] J. Hata and I. P. Grant, *J. Phys. B* **16**, 3713 (1983).
- [46] I. P. Grant, *Int. J. Quantum Chem.* **25**, 23 (1984).
- [47] K. G. Dyall, I. P. Grant, C. T. Johnson, F. A. Parpia, and E. P. Plummer, *Comput. Phys. Commun.* **55**, 425 (1989).
- [48] J. A. Bearden, *Rev. Mod. Phys.* **39**, 78 (1967).
- [49] S. I. Salem and P. L. Lee, *At. Data Nucl. Data Tables* **18**, 233 (1976).